

Original Research

Very Low Doses of *Mycobacterium tuberculosis* Yield Diverse Host Outcomes in Common Marmosets (*Callithrix jacchus*)

Anthony M Cadena,¹ Edwin C Klein,² Alexander G White,¹ Jaime A Tomko,¹ Chelsea L Chedrick,¹ Douglas S Reed,³ Laura E Via,^{4,5} Philana Ling Lin,⁶ and JoAnne L Flynn,^{1,*}

Identifying and refining small-animal models of tuberculosis that recapitulate aspects of human *Mycobacterium tuberculosis* infection can contribute to advancing our understanding of critical facets of the disease. To study the effects of very low-dose infections with 2 strains of *M. tuberculosis* on disease progression and survival in common marmosets, animals were challenged with strains Erdman and CDC1551 at doses ranging from 1 to 12 cfu. These data revealed that the susceptibility of marmosets to *M. tuberculosis* infection is influenced by strain virulence and initial dose. Marmoset infection with the Erdman strain, even at very low doses, resulted in rapid disease progression associated with severe weight loss, extensive pathology, and poor survival. By contrast, challenge with the less virulent CDC1551 strain resulted in slower disease progression, delayed weight loss, and prolonged survival. One marmoset infected with CDC1551 at a very low dose (approximately 1 cfu) was able to contain and control *M. tuberculosis* infection in a subclinical state that persisted as long as 300 d. These findings underscore the critical importance of understanding the heterogeneity in host outcome that can arise in association with different infectious doses and strains in the marmoset model of tuberculosis.

Abbreviation: PET–CT, ¹⁸F-fluorodeoxyglucose positron-emission tomography–CT imaging

Tuberculosis remains a risk to global public health, with 9.6 million new cases of active tuberculosis and 1.5 million deaths in 2014.²³ Although most humans contain *Mycobacterium tuberculosis* in a clinically asymptomatic infection termed ‘latent tuberculosis,’ a smaller subset (approximately 10%) of patients present initially with primary active disease or subsequent disease reactivation over the course of their lifetime.¹⁸ The biologic basis for the disease spectrum of *M. tuberculosis* in humans is unknown and continues to be an active area of research.

Several animal models have been adapted for experimental *M. tuberculosis* infection, greatly contributing to our understanding of tuberculosis biology.⁸ NHP models of tuberculosis, particularly cynomolgus macaques (*Macaca fascicularis*)^{3,15} and rhesus macaques (*Macaca mulatta*),^{4,20} are recognized as the most faithful animal models in replicating the human spectrum of disease in terms of both pathology and infection outcome.^{3,9,12,13} In addition,

the recently developed common marmoset model of tuberculosis (*Callithrix jacchus*)²² replicates crucial facets of human tuberculosis, including cavitory disease. This model demonstrated divergent rates of disease progression after challenge with 3 strains—a Beijing isolate, the less virulent strain CDC1551, and *M. africanum*—and 2 different inocula (250 and 25 cfu). Notably, each infection resulted in rapid pulmonary disease presentation and weight loss, and all animals died by 75 d after challenge, thus reflecting the inherent susceptibility of common marmosets to this infection.

The influence of *M. tuberculosis* dose and strain on host outcome has been examined in several animal models. For example, BALB/c mice demonstrated a broad range of virulence, bacterial load, and pathology after infection with 19 different *M. tuberculosis* complex strains of 11 major genotype families.⁷ These 19 strains were segregated according to their virulence, bacterial burden, pathology, and delayed-type hypersensitivity responses as high, intermediate, and low responders. Strains that were classified as high responders induced the most pathology, greatest bacterial burden and highest mortality and included the isolates Beijing 2 and 3, Africa 2, and Somalia 2. At the other end of the spectrum, those strains that elicited the least severe pathologic scores caused no or minimal mortality after 112 d, yielded the lowest bacterial load, and included the isolates H37Rv, Canetti, and Beijing 1.⁷ A recent review examined the virulence and immunogenicity of several genotypic lineages of *M. tuberculosis* in

Received: 05 Jan 2016. Revision requested: 15 Feb 2016. Accepted: 28 Apr 2016.

¹Department of Microbiology and Molecular Genetics, ³Center for Vaccine Research, Department of Immunology, University of Pittsburgh School of Medicine, Pittsburgh, Pennsylvania; ²Division of Laboratory Animal Research, University of Pittsburgh, Pittsburgh, Pennsylvania; ⁴Tuberculosis Research Section, National Institute of Allergy and Infectious Diseases, NIH, Bethesda, Maryland; ⁵Institute of Infectious Disease and Molecular Medicine, Department of Pathology, University of Cape Town, Cape Town, South Africa; and ⁶Division of Infectious Diseases, Department of Pediatrics, Children’s Hospital of Pittsburgh of UPMC, University of Pittsburgh School of Medicine, Pittsburgh, Pennsylvania.

*Corresponding author. Email: joanne@pitt.edu

mice and related these findings to observed human epidemiologic data.¹⁰ Overall, virulence and immune response vary extensively within each genotype, with many genotypes having both high- and low-virulence variants. Furthermore, rabbits (like mice) demonstrate an influence of dose, strain, and growth phase on tubercle formation and virulence, and *M. tuberculosis* strain Erdman had the greatest virulence in rabbits, requiring the fewest inhaled bacilli to generate visible tubercles at 5 wk.¹⁶

Whether common marmosets have any capacity to control *M. tuberculosis* infection or are universally susceptible to developing active tuberculosis, even with low-dose inocula, has not been determined to date. In this study, we aimed to better characterize the disease phenotypes and host outcomes of common marmosets after *M. tuberculosis* infection by challenging animals with very low doses (less than 15 cfu) of the Erdman and CDC1551 strains.

Materials and Methods

Animals. Common marmosets (*Callithrix jacchus*) were obtained from the Wisconsin National Primate Research Center (Madison, WI). Prior to shipment, the animals were tested for *Campylobacter*, *Shigella*, *Salmonella*, *Giardia*, *Cryptosporidium*, *Entamoeba*, and *Balantidium*. On arrival at the University of Pittsburgh, the marmosets were screened for *M. tuberculosis* infection and other comorbidities during a month-long quarantine. More specifically, each macaque underwent complete baseline blood and biochemical analyses, 2 tape tests to screen for pinworms, and *Giardia* ELISA with 2 pooled fecal sets. All marmosets were housed and maintained according to the practices and standards detailed in the Animal Welfare Act² and the *Guide for the Care and Use of Laboratory Animals*¹¹ within a biosafety level 3 facility. These NHP were housed in a 4 × 4 macaque cage system, with the internal dividers removed to allow for open access and opportunities for climbing to the top and bottom of the cage. A nest box was included in the upper part of the cage, and the animals were fed a specialized marmoset diet (as advised by Dr Saverio Capuano, Wisconsin Primate Center). In some cases, infected animals were cohoused with naïve cagemates for a separate transmission study. The IACUC at the University of Pittsburgh approved all protocols and experiments.

Infection and necropsy. Common marmosets were infected with either the virulent Erdman strain of *M. tuberculosis* or CDC1551 at doses of 1 to 12 cfu, as determined by plating the inoculum. One animal in the Erdman cohort was infected by aerosol, and the remaining marmosets were infected through bronchoscopic instillation, as previously described.³ In brief, a disinfected bronchoscope was placed into the desired bronchus and 0.2 mL of sterile saline containing the appropriate infection inoculum was instilled. For the marmoset infected by aerosol, an infection inoculum was administered through a 10-min exposure to aerosolized bacilli created by a 3-jet Collision nebulizer (BGI, Waltham, MA) controlled by the AeroMP bioaerosol exposure system (Biaera Technologies, Hagerstown, MD) in a head-only exposure chamber (CH Technologies, Westwood, NJ) within a class III biologic safety cabinet (Baker, Sanford, ME). After infection, all marmosets were clinically monitored for signs of infection according to previously published methods,^{3,15} and ¹⁸F-fluorodeoxyglucose positron-emission tomography–CT (PET–CT) scans were performed monthly, as previously described.^{5,6,22} Marmosets were euthanized when they lost more than 20% of their preinfection body weight or when they exhibited substantial clinical signs of

disease (for example, lethargy and anorexia). At necropsy, a gross pathology score for each marmoset was determined according to our published scoring system,¹⁵ which evaluates tuberculosis-specific disease in all lung lobes, thoracic lymph nodes, and extrapulmonary sites. Overall bacterial burden scores and cfu counts for individual granulomas, regions of complex pathology (for example, tuberculosis pneumonia), and thoracic lymph nodes were quantified and calculated as previously described.^{14,15} Briefly, multiple individual tissue samples in each marmoset were identified by using PET–CT imaging as a guide, excised, and plated at necropsy, and bacterial colonies were counted 21 d after necropsy. The cfu score for each animal was determined by summation of each tissue's log-transformation of bacterial burden, thus providing a relative comparator for all marmosets. In comparison, the total cfu count was the sum of the actual number of bacilli in all samples taken from the animal, and thus provided a more accurate representation of the bacterial burden.

Results

Host outcome and survival after *M. tuberculosis* infection in marmosets. To determine the clinical progression and disease pathology of very low-dose infection, 9 marmosets were challenged with 2 different strains of *M. tuberculosis* at doses of 1 to 12 cfu (Table 1). Inocula were determined by plating at the time of challenge. All but one of the marmosets in this study were infected by direct instillation of bacteria into the airways by using a bronchoscope. The marmoset that received 12 cfu of the Erdman strain (animal no. 3012) was infected through aerosol dispersion. All marmosets infected with the Erdman strain (dose range, 1 to 12 cfu, with most animals infected with 2 cfu) presented with rapidly progressing disease regardless of dose. Clinically, all of these marmosets exhibited physical signs of illness, including inactivity, reclusiveness, and diminished appetite. The animals exhibited precipitous weight loss after infection and arrived at the weight-loss threshold of 20% by 45 d after infection (median, 39 d), requiring euthanasia (Figure 1). Coughing was observed in a subset of animals (marmosets 13210, 13310, 13410, 13610, 13710, and 3412). At necropsy, all animals infected with strain Erdman had gross pathology scores that exceeded 30 (median score, 41; Table 1).

By contrast, the 2 marmosets challenged with strain CDC1551 (dose, 1 or 7 cfu) had divergent outcomes associated with dose but demonstrated reduced overall disease compared with that of marmosets infected with strain Erdman. The marmoset that received 7 cfu of the CDC1551 strain (animal no. 3913) had mild to moderate disease progression and steady weight loss and survived to 89 d (Table 1 and Figure 1). Surprisingly, the marmoset that received 1 cfu of CDC1551 (animal no. 3713) had mild disease progression, with a sustained period of weight loss in this animal beginning on day 76 that was not accompanied by any other clinical signs of disease. By day 174, this marmoset was regaining weight and returned to its initial weight by day 282 (Figure 1). This marmoset was euthanized after the conclusion of the study on day 307; euthanasia was not due to weight loss or clinical morbidity. The marmoset inoculated with 7 cfu had a gross pathology score of 66, whereas the marmoset inoculated with 1 CFU had a score of 25 (Table 1).

In vivo PET–CT imaging. To compare in vivo disease progression between strains and doses, all marmosets were followed by using serial PET–CT imaging;^{5,6} we here present 2 representative

Table 1. Survival, disease presentation, and bacterial burden and dissemination after infection of common marmosets with very low doses of *M. tuberculosis*

Animal no.	Bacterial strain	Infection dose (no. of cfu)	Survival (d)	Gross pathology score	CFU score	% of tissue samples containing bacteria
13210	Erdman	2	39	49	142	100
13310		2	35	56	164	100
13410		2	37	41	158	100
13610		2	38	31	123	100
13710		2	40	33	137	95.2
3012		12	32	53	144	100
3412		1	43	33	107	100
3713	CDC1551	1	307	25	26	32
3913		7	89	66	53	100

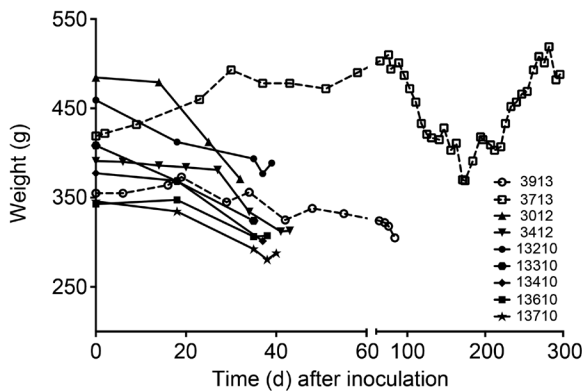


Figure 1. Weight loss after infection with very low doses of *M. tuberculosis* varied according to strain and dose. All animals except one had sustained weight loss that prompted euthanasia by 90 d. The marmoset infected with 1 cfu of CDC1551 (animal no. 3713) had a period of weight loss but recovered its preinfection body weight by day 282. This animal was euthanized at 307 d after infection due to the conclusion of the study.

animals from each cohort for comparison. For strain Erdman, 2 marmosets (nos. 3012 and 3412) were imaged and compared with 2 animals infected with CDC1551 (nos. 3913 and 3713). Both sets of animals represented the highest and lowest dose administered for each strain (Table 1). In agreement with clinical and weight observations, these marmosets had differing rates of disease progression, as demonstrated by ¹⁸F-fluorodeoxyglucose uptake. Relative to their baseline scans, both Erdman-infected marmosets had activity indicative of pulmonary and lymphatic disease on their 4-wk postinfection PET-CT scans (Figure 2, yellow arrows), whereas the 2 animals challenged with CDC1551 had normal scans without disease, thus reflecting the slower progression associated with this strain. The preneopsy scan for each animal was obtained just a few days prior to euthanasia. Given the rapid loss of body weight that necessitated early euthanasia in the 2 Erdman-infected marmosets, the 4-wk scans served as their preneopsy scans. By contrast, the disease in the CDC1551-infected marmosets progressed more slowly (preneopsy scans at weeks 12 and 44). In particular, marmoset 3913 had significant disease in the right lower lung lobe and thoracic lymph nodes (Figure 2, yellow arrows), and marmoset 3713 (dose, 1 cfu of CDC1551) had

very little ¹⁸F-fluorodeoxyglucose uptake during his preneopsy scan at 300 d after infection.

Overall bacterial burden and extent of dissemination. Comparisons of bacterial burden (cfu scores)¹⁵ and the number of bacteria per tissue sample (granuloma, lymph node, tuberculosis pneumonia)¹⁴ revealed strain- and dose-dependent differences dependent (Table 1 and Figure 3). All of the Erdman-infected marmosets (including the one that received a dose of 1 cfu) had cfu scores above 100 (median, 142) and more than 95% of the tissues cultured were positive for *M. tuberculosis* (Table 1), indicative of prominent and widespread disease. By contrast, the 2 marmosets challenged with 7 and 1 cfu of CDC1551 had cfu scores of 53 and 26, respectively, supporting the finding that bacterial burden is related to dose for this strain (Figure 3 A). The inoculation dose of 7 cfu of CDC1551 resulted in 100% of tissues that were positive for tubercular bacilli, whereas the infection due to the 1-cfu dose was contained to a much greater extent, with only 32% of tissues positive for bacteria (Table 1). Two marmosets from the Erdman group (no. 3012, inoculated with 12 cfu, and no. 3412, which received 1 cfu) were selected for more precise comparison of tissue burden with the 2 animals infected with CDC1551 (marmosets 3913 and 3713). Comparisons of each animal's cumulative bacterial burden (total cfu counts among all lung and lymph node samples) revealed that 3 of the marmosets had cumulative burdens that exceeded 5×10^6 cfu, with little difference between the lung and lymph-node compartments (Figure 3 B). In contrast, the total bacterial load in the marmoset infected with 1 cfu of CDC1551 (no. 3713) was nearly 100-fold lower than that in the other 3 (Figure 3 B), with the vast majority of the burden contributed by infected thoracic lymph nodes (Figure 3 C). Assessing each tissue separately revealed that the median lung or lymph node bacterial burden was higher in the 2 animals that received the higher dose within each strain (Figure 3 C). Lymph nodes had the greatest variability across the different tissues, and the highest burdens occurred in regions of lung tuberculosis pneumonia. Most notably, the tissue bacterial burden in the marmoset that received 1 cfu of CDC1551 ranged from primarily sterile sites to the moderately infected superior pretracheal lymph node, which had 6.4×10^4 cfu.

Gross and histologic disease pathology after challenge with very low doses of *M. tuberculosis*. Comparison of gross pathology at necropsy (Figure 4) revealed marked differences in the magnitude and extent of disease progression. For example, marmoset 3412,

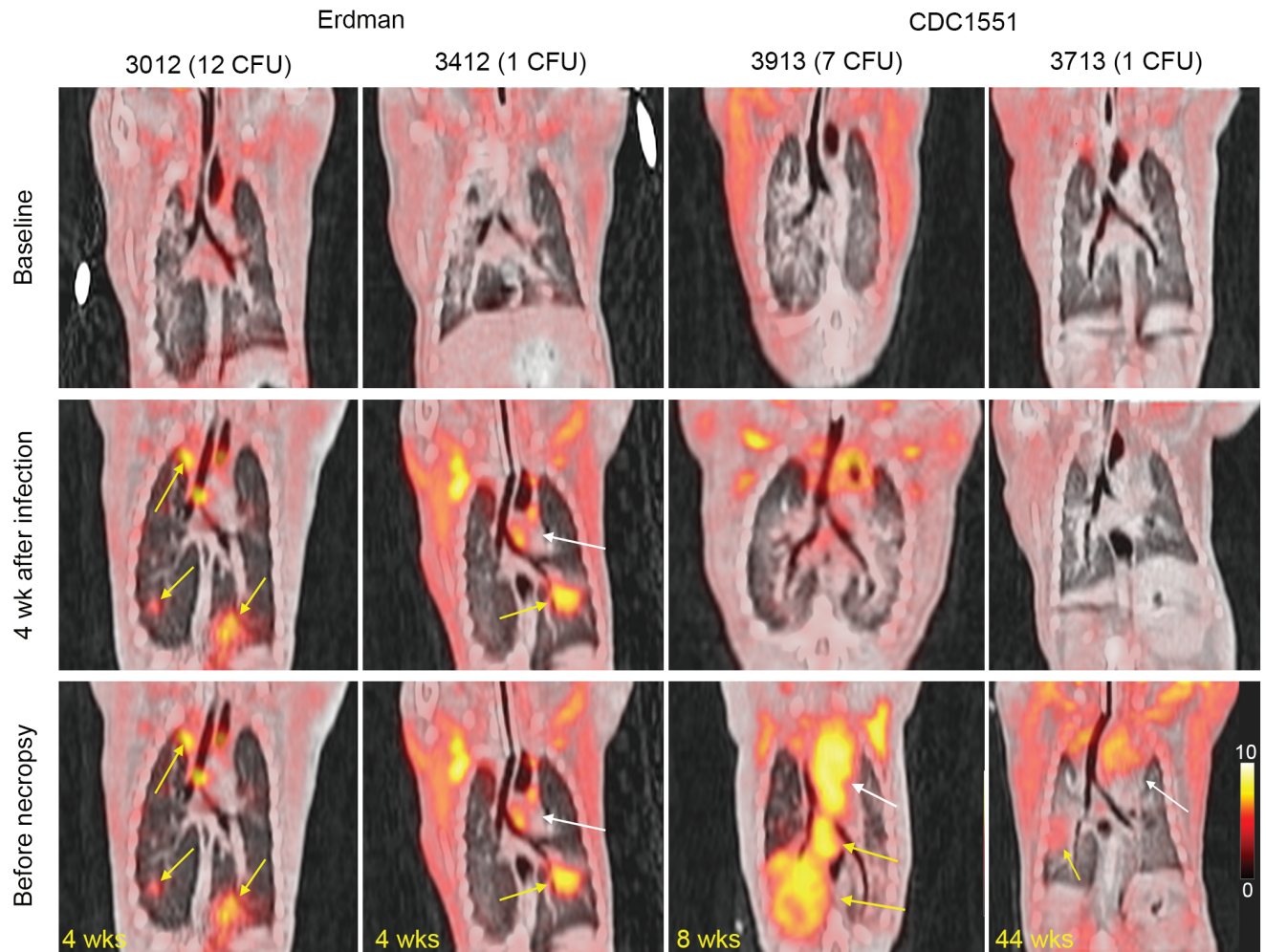


Figure 2. Serial PET–CT imaging of infected marmosets revealed variable disease progression that was dependent on dose. These images are representative PET–CT coronal cross-sections from marmosets infected with very low doses *M. tuberculosis*; ^{18}F -fluorodeoxyglucose was used as a probe for inflammation. Left panel: 2 marmosets infected with the Erdman strain (doses, 12 and 1 cfu) were followed over the course of infection. For both animals, their 4-wk scans served as their pre-necropsy scans, in light of their rapid disease progression and clinical decline. Right panel: 2 marmosets infected with CDC1551 (doses, 7 and 1 cfu) were followed throughout infection. For all animals, the date of each pre-necropsy scan (in weeks) is labeled at the lower left. Yellow arrows denote diseased areas of lung and thoracic lymph nodes, whereas the white arrow highlights noninflammatory uptake in the heart.

which was infected with 1 cfu of the Erdman strain, demonstrated pulmonary disease that was grossly limited to the left lower lung (Figure 4 A), with concomitant enlargement and effacement of the left thoracic lymph nodes (Figure 4 B). The left lower lobe showed extensive tuberculous pneumonia, with a central focal area of severe necrotizing consolidation (2 cm); the lobe completely lacked any normal, aerated lung parenchyma. Gross examination of the spleen and liver revealed enlargement of both organs, with numerous (20 or more) granulomas (diameter, pinpoint to 1 mm or greater) throughout (Figure 4 C).

By contrast, gross examination of tissues from the marmoset infected with 1 cfu of CDC1551 (no. 3713) revealed 2 relatively well-circumscribed lesions in the left (lesion diameter, 1.5 mm) and right (10 mm) lower lobes (Figure 4 D); there were 4 additional discrete lesions (diameter, 2 mm or less) in the right lower lobe. The inferior and superior pretracheal lymph nodes were both enlarged, with significant effacement in the superior node (Figure 4 E). The liver (Figure 4 F) and spleen had no readily

identifiable gross lesions. The liver was markedly enlarged, extending several centimeters below the costal region, and had an accentuated lobular appearance, with several large, irregular, superficial regions of parenchymal pallor. This discoloration was likely due to differential blood settling, euthanasia-solution-induced hepatocellular artifact, or glycogenation; there was no gross indication of tuberculosis throughout this organ.

Histopathology of lung, thoracic lymph nodes, spleen, and liver largely confirmed the findings at necropsy. For the marmoset challenged with 1 cfu of the Erdman strain (animal 3412), the region of tuberculosis pneumonia in the left lower lobe consisted of extremely neutrophil-rich inflammatory infiltrate, extending from alveolus to alveolus. Centrally, there was a large area of coagulative necrosis with near total effacement of all recognizable tissue architecture. There was minimal evidence of the formation of architecturally organized granuloma structures per se within the entirety of the large necrotizing region (Figure 5 A). The left

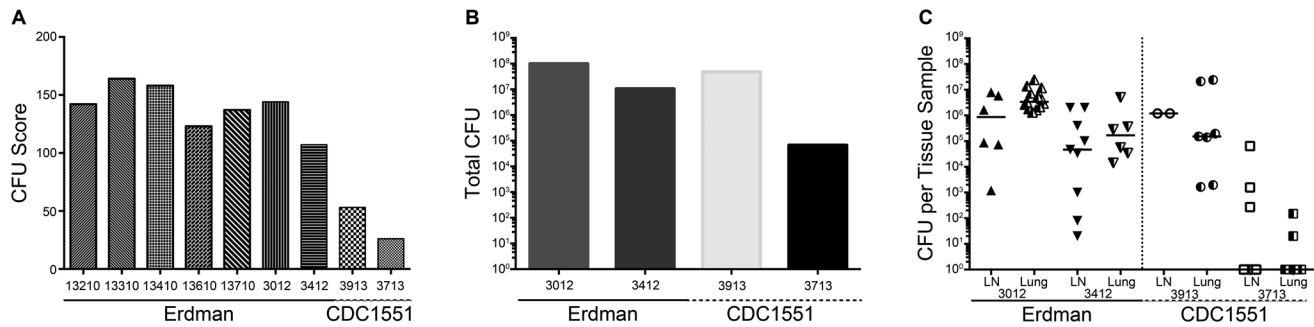


Figure 3. Very low dose infection with CDC1551 results in diminished bacterial burden. (A) Comparisons of cfu scores for all 7 marmosets reveal the decreased scores for the 2 animals that received CDC1551. (B) Total cfu counts (the sum of all bacilli from every plated sample) and (C) the number of cfu per tissue sample from a subset of marmosets reveal the reduced bacterial loads in the 2 marmosets infected with CDC1551. In the marmoset infected with 1 cfu of CDC1551 (animal no. 3713), the total bacterial burden was approximately 2 logs lower than that in any other animal, and there were fewer bacilli in individual tissues, with a majority of samples being sterile.



Figure 4. Gross pathology after infection with very low doses of CDC1551 was reduced relative to that after Erdman. Representative gross pathology from 2 marmosets infected with 1 cfu of the Erdman strain (top row) and 1 cfu of CDC1551 (bottom row). These images show the major disease-associated differences between the 2 animals. (A) Left lower lobe of lung with a central consolidation. (B) Enlarged and effaced left cranial hilar and left main-stem bronchial nodes, with mildly swollen central carinal lymph nodes. (C) Enlarged spleen and liver, with many disseminated pinpoint granulomas. (D) Granuloma in right lower lobe of lung. (E) Enlarged superior pretracheal lymph nodes. (F) Liver without gross evidence of tuberculous disease. Black arrows highlight areas of tuberculous disease.

cranial hilar lymph node displayed extensive nodal effacement, with regions of necrotizing and nonnecrotizing inflammation with poor structural organization (Figure 5 B). Examination of the spleen (Figure 5 C) and liver (Figure 5 D) revealed multiple regions of caseous and nonnecrotizing granulomas, indicative of widespread disseminated disease.

In the marmoset challenged with 1 cfu of CDC1551 (animal 3713), the left lower lung lobe contained a single, caseous granuloma

that was well circumscribed and had a prominent lymphocytic cuff (Figure 5 D). In contrast to lung, the superior pretracheal lymph node had prominent coalescing and effacing caseous granulomas, with evidence of early collagen fibril formation within the necrotic matrix (Figure 5 E). Despite the lack of gross disease at necropsy, this marmoset had microscopic evidence of splenic tuberculosis, with multiple, small minimally necrotizing granulomas (Figure 5 F). In addition, sections of liver exhibited several

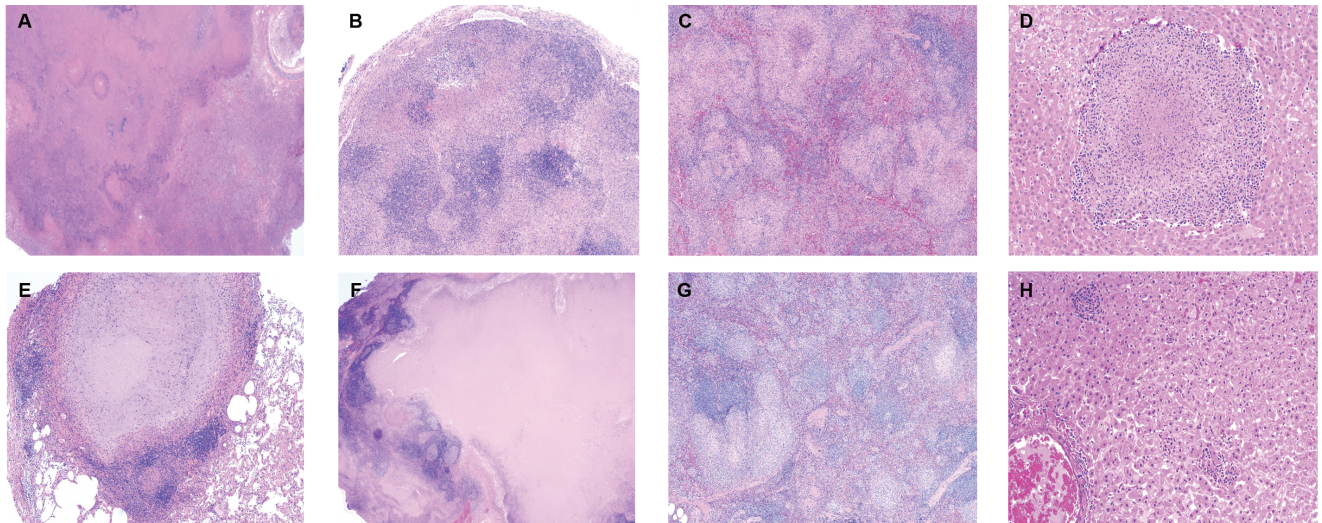


Figure 5. Histopathology after infection with very low doses of the Erdman and CDC1551 strains. Representative histopathology from the 2 marmosets shown in Figure 4, which were infected with 1 cfu of the Erdman strain (top row) and 1 cfu of CDC1551 (bottom row). These images illustrate the differences between the 2 animals, particularly in the organization and structure of the lung granulomas. (A) Tuberculosis pneumonia with a large area of necrosis in the left lower lung lobe; magnification, 1.25 \times . (B) Left cranial hilar lymph node with areas of necrotizing and nonnecrotizing granulomatous inflammation; magnification, 4 \times . (C) Spleen with disseminating necrotizing and nonnecrotizing foci; magnification, 4 \times . (D) Liver with caseous granuloma; magnification, 10 \times . (E) Circumscribed caseous granuloma with a well defined lymphocytic cuff in the left lower lung lobe; magnification, 4 \times . (F) Superior pretracheal lymph node with coalescing and effacing caseous granulomas; magnification, 4 \times . (G) Spleen with multiple areas of minimally necrotizing granulomas dispersed throughout the parenchyma; magnification, 4 \times . (H) Liver with several, small sinusoidal nonnecrotizing granulomas; magnification, 10 \times . Hematoxylin and eosin stain.

focal areas containing caseous granulomas and small, nonnecrotizing sinusoidal granulomas (Figure 5 F).

Overall, the gross and microscopy pathology mirrored the clinical differences in these 2 marmosets and reiterate the distinction between the 2 strains, even at very low doses. Similar extensive gross and microscopic disease was present in all marmosets infected with the Erdman strain as well as in the animal infected with 7 cfu of strain CDC1551. Importantly, despite the marked difference in the general histologic appearance between the 2 CDC1551-infected animals and the more immunologically contained response in the marmoset challenged with 1 cfu, this marmoset had numerous microscopic findings that suggested that the disease was entering a more widely disseminating stage. The presence of numerous small nonnecrotizing granulomas and epithelioid cell aggregates within thoracic lymph nodes as well as the microscopic granulomas in the hepatic and splenic parenchyma indicated the onset of more fulminant and progressive disease prior to necropsy.

Discussion

Here we report the diverse disease progression and host outcome patterns that occurred after the infection of common marmosets with very low doses (1 to 12 cfu) of 2 strains of *M. tuberculosis*. The susceptibility of marmosets to the Erdman strain was unrelated to dose or route. However, the inoculation dose may be an important determinant of outcome after challenge with the less virulent CDC1551 strain. All of the marmosets challenged with low doses of strain Erdman presented with fulminant, disseminating active tuberculosis, had a median survival time of 39 d, and had evidence of invasive necrotizing alveolitis and tuberculosis pneumonia, with little evidence of well-circumscribed granulomas. In contrast, infection with CDC1551 promoted a

more slowly progressing infection overall; the marmoset that received 7 cfu survived to 89 d, and the animal given 1 cfu survived more than 300 d. To our knowledge, this is the first reported instance of apparent recovery, stabilization, and survival beyond 300 d of a marmoset infected with a strain of *M. tuberculosis*.

Our initial findings recapitulated those reported by our colleagues, who also described differential disease progression between several strains within the *M. tuberculosis* complex.²² This previous study compared CDC1551, *M. africanum* N0091, and a Beijing K04 isolate at doses of 25 and 250 cfu; all 3 strains at both doses produced fulminant disease and prompted euthanasia by 80 d after infection due to weight loss.²² The rapid disease progression, high bacterial burden, and invasive necrotizing pathology associated with the Beijing K04 isolate is very similar to the disease evolution, bacterial load, and disease presentation in our marmosets that were infected with the virulent Erdman strain. The median survival time in the previous study was 37 d,²² similar to the 39 d for Erdman-infected marmosets in the current study. Moreover, the higher dose of the K04 isolate was the only case for which the rate of weight loss was significantly increased. Likewise, among the Erdman-infected marmosets in our study, the animal that received 12 cfu had the most rapid weight decline and was euthanized 32 d after infection. In contrast, infection with CDC1551 resulted in the slowest disease progression among the 3 strains evaluated previously and yielded a median survival time of 59 d.²² Notably, half of the marmosets infected with the CDC1551 strain previously developed cavitory lesions, a particular manifestation of human tuberculosis that is associated with erosion of lung parenchyma into the airway, facilitating bacterial transmission.¹⁹ In agreement with these findings, our marmoset that received 7 cfu of CDC1551 (no. 3913) demonstrated several sites of cavitation. A separate study performed by these collaborators^{21,22} followed marmosets infected with various low aerosol

doses of CDC1551 for weight loss in infected animals prior to drug treatment at 7 wk. Little to no weight loss was seen in the animals exposed to 1 to 2 CFU, whereas infection with higher doses significantly increased weight loss percentage (data not shown) suggesting that the route of infection was not directly responsible for the difference observed in the marmoset infected with 1 CFU of CDC1551 presented here.

Extending the published findings, we present data supportive of long-term control of infection in a single marmoset. Infection with approximately 1 cfu of CDC 1551 presented as 2 primary lesions, one in each of the lower lung lobes, as determined by PET-CT imaging^{5,6} (Figure 2). Except for a period of transient weight loss beginning at day 76 after infection, this marmoset showed no other sign of clinical morbidity. Close observation by PET-CT imaging revealed that the lesion in the right lower lobe gradually increased in tracer uptake, whereas the signal in the lesion in the opposite lobe gradually decreased, suggesting at least partial immunologic control and disease resolution. This apparent discrepancy between the 2 individual lesions is characteristic of the independent nature of granulomas even within the same NHP host.^{6,14} These results were confirmed at necropsy, in that the lesion in the left lower lobe was sterile (that is, yielded no organisms by plating), whereas the lesion in the right lower lobe had approximately 2.6×10^3 bacteria. However, the microscopic pathology in the nodal lymph nodes and the presence of microscopic granulomas in the liver and spleen suggest that the infection may have been entering a more invasive stage, albeit at a slower rate than reported for all other marmosets to date. The histologic characteristics of the 2 lung lesions from this animal were distinct from the granulomas excised from the marmoset infected with 7 cfu of the same strain and from any of marmosets challenged with the Erdman strain. The left lower lobe lesion was an archetypical caseous granuloma with a well-circumscribed lymphocytic cuff, whereas the right lower lobe lesion had areas of tuberculosis pneumonia and nonnecrotizing granulomas. All of the Erdman-infected animals had a predominance of invasive, neutrophil-rich granulomatous alveolitis in their pulmonary sites that exhibited occasional organization and circumscription but did not form traditional defined granulomatous structures. Overall, the recovery of body weight and the lack of clinical manifestations coupled with the postmortem observations of decreased total cfu counts, diminished bacterial dissemination, and less extensive gross pathology suggest that the marmoset's greater capacity to limit disease progression was likely due to the reduced virulence of CDC1551 and the very low infection dose.

The primary limitation of our study is that the stable but chronic infection phenotype has only been observed in the single marmoset described. However, we found a strong relationship between the infectious dose of CDC1551 and weight loss in marmosets. Further infections with 1 to 3 cfu of CDC1551 are warranted in this small animal model to better define the mechanisms of control of low-dose infection. If this NHP species does exhibit relative resistance to *M. tuberculosis* in a persistent manner, it would broaden their applicability as a small animal model of tuberculosis to include chronic infection studies yet retain their inherent benefits as a NHP model that offers decreased cost, small size,¹⁷ dizygotic twinning,¹ pliability for drug studies,²¹ and the ability to replicate aspects of human disease.^{17,22} In addition, marmosets might be developed as a model for vaccine-induced protection against tuberculosis.

In conclusion, optimizing the common marmoset (*C. jacchus*) model of *M. tuberculosis* infection requires identification of the range of host outcomes for this NHP species. In the current study, we noted variable disease progression in marmosets challenged with very low doses (1 to 12 cfu) of 2 strains of *M. tuberculosis*. Both the dose and strain of *M. tuberculosis* influenced the outcomes after challenge. Very low-dose challenge with the virulent Erdman strain did not ameliorate the rate of disease progression, because all of these marmosets (even those infected with 1 to 2 cfu) presented with rapidly disseminating active disease, resulting in clinical decline that prompted euthanasia by 43 d after inoculation. Infection with the less virulent CDC1551 strain resulted in delayed disease progression that was somewhat dependent on the inoculation dose. One of the most striking findings was that challenge with approximately 1 cfu of CDC1551 produced one case in which a marmoset effectively controlled the *M. tuberculosis* infection in a subclinical state for more than 300 d. At necropsy, this marmoset had reduced bacterial burden in its involved lymph nodes and lungs, reduced tissue dissemination, less overt gross pathology, and mildly progressing histology. These findings are in stark contrast to all previously reported *M. tuberculosis* infections of common marmosets, thus potentially extending this small-animal model beyond studies of acute infection while maintaining the clinical spectrum observed in the human disease.

Acknowledgments

We thank Mark Rodgers, Carolyn Bigbee, Catherine Cochran, and Charles Scanga for technical assistance. We also thank Daniel Filmore for veterinary and animal assistance. We gratefully acknowledge Pauline Maiello and Teresa Coleman for imaging support and Danielle Weiner, Daniel Schimel, and Manny Dayao for veterinary assistance at NIAID. These studies were funded in part by a NIH training grant (T32 AI089443 [to AMC]), the Bill and Melinda Gates Foundation (grant no. OPP1034408 [to JLF]), and the intramural research program of NIAID, NIH (to LEV).

References

1. Abbott DH, Barnett DK, Colman RJ, Yamamoto ME, Schultz-Darken NJ. 2003. Aspects of common marmoset basic biology and life history important for biomedical research. *Comp Med* 53:339-350.
2. Animal Welfare Act as Amended. 2008. 7 USC §2131-2156.
3. Capuano SV 3rd, Croix DA, Pawar S, Zinovik A, Myers A, Lin PL, Bissel S, Fuhrman C, Klein E, Flynn JL. 2003. Experimental mycobacterium tuberculosis infection of cynomolgus macaques closely resembles the various manifestations of human m. tuberculosis infection. *Infect Immun* 71:5831-5844.
4. Chen CY, Huang D, Wang RC, Shen L, Zeng G, Yao S, Shen Y, Halliday L, Fortman J, McAllister M, Estep J, Hunt R, Vasconcelos D, Du G, Porcelli SA, Larsen MH, Jacobs WR Jr, Haynes BF, Letvin NL, Chen ZW. 2009. A critical role for CD8 T cells in a nonhuman primate model of tuberculosis. *PLoS Pathog* 5:e1000392.
5. Coleman MT, Chen RY, Lee M, Lin PL, Dodd LE, Maiello P, Via LE, Kim Y, Marriner G, Dartois V, Scanga C, Janssen C, Wang J, Klein E, Cho SN, Barry CE 3rd, Flynn JL. 2014. PET/CT imaging reveals a therapeutic response to oxazolidinones in macaques and humans with tuberculosis. *Sci Transl Med* 6:265ra167.
6. Coleman MT, Maiello P, Tomko J, Frye LJ, Fillmore D, Janssen C, Klein E, Lin PL. 2014. Early changes by (18)Fluorodeoxyglucose positron emission tomography coregistered with computed tomography predict outcome after Mycobacterium tuberculosis infection in cynomolgus macaques. *Infect Immun* 82:2400-2404.
7. Dormans J, Burger M, Aguilar D, Hernandez-Pando R, Kremer K, Roholl P, Arend SM, van Soolingen D. 2004. Correlation of

- virulence, lung pathology, bacterial load and delayed type hypersensitivity responses after infection with different *Mycobacterium tuberculosis* genotypes in a BALB/c mouse model. *Clin Exp Immunol* **137**:460–468.
8. Flynn JL. 2006. Lessons from experimental *Mycobacterium tuberculosis* infections. *Microbes Infect* **8**:1179–1188.
 9. Flynn JL, Chan J, Lin PL. 2011. Macrophages and control of granulomatous inflammation in tuberculosis. *Mucosal Immunol* **4**:271–278.
 10. Hernandez-Pando R, Marquina-Castillo B, Barrios-Payan J, Mata-Espinosa D. 2012. Use of mouse models to study the variability in virulence associated with specific genotypic lineages of *Mycobacterium tuberculosis*. *Infect Genet Evol* **12**:725–731.
 11. Institute for Laboratory Animal Research. 2011. Guide for the care and use of laboratory animals, 8th ed. Washington (DC): National Academies Press.
 12. Kaushal D, Mehra S, Didier PJ, Lackner AA. 2012. The nonhuman primate model of tuberculosis. *J Med Primatol* **41**:191–201.
 13. Lin PL, Flynn JL. 2010. Understanding latent tuberculosis: a moving target. *J Immunol* **185**:15–22.
 14. Lin PL, Ford CB, Coleman MT, Myers AJ, Gawande R, Ioerger T, Sacchetti J, Fortune SM, Flynn JL. 2014. Sterilization of granulomas is common in active and latent tuberculosis despite within-host variability in bacterial killing. *Nat Med* **20**:75–79.
 15. Lin PL, Rodgers M, Smith L, Bigbee M, Myers A, Bigbee C, Chiosea I, Capuano SV, Fuhrman C, Klein E, Flynn JL. 2009. Quantitative comparison of active and latent tuberculosis in the cynomolgus macaque model. *Infect Immun* **77**:4631–4642.
 16. Manabe YC, Dannenberg AM, Tyagi SK, Hatem CL, Yoder M, Woolwine SC, Zook BC, Pitt MLM, Bishai WR. 2003. Different strains of *Mycobacterium tuberculosis* cause various spectrums of disease in the rabbit model of tuberculosis. *Infect Immun* **71**:6004–6011.
 17. Mansfield K. 2003. Marmoset models commonly used in biomedical research. *Comp Med* **53**:383–392.
 18. O'Garra A, Redford PS, McNab FW, Bloom CI, Wilkinson RJ, Berry MP. 2013. The immune response in tuberculosis. *Annu Rev Immunol* **31**:475–527.
 19. Ong CW, Elkington PT, Friedland JS. 2014. Tuberculosis, pulmonary cavitation, and matrix metalloproteinases. *Am J Respir Crit Care Med* **190**:9–18.
 20. Verreck FA, Vervenne RA, Kondova I, van Kralingen KW, Remarque EJ, Braskamp G, van der Werff NM, Kersbergen A, Ottenhoff TH, Heidt PJ, Gilbert SC, Gicquel B, Hill AV, Martin C, McShane H, Thomas AW. 2009. MVA.85A boosting of BCG and an attenuated, *phoP* deficient *M. tuberculosis* vaccine both show protective efficacy against tuberculosis in rhesus macaques. *PLoS One* **4**:e5264. Erratum in: *Plos One* 2011.
 21. Via LE, England K, Weiner DM, Schimel D, Zimmerman MD, Dayao E, Chen RY, Dodd LE, Richardson M, Robbins KK, Cai Y, Hammoud D, Herscovitch P, Dartois V, Flynn JL, Barry CE 3rd. 2015. A sterilizing tuberculosis treatment regimen is associated with faster clearance of bacteria in cavitary lesions in marmosets. *Antimicrob Agents Chemother* **59**:4181–4189.
 22. Via LE, Weiner DM, Schimel D, Lin PL, Dayao E, Tankersley SL, Cai Y, Coleman MT, Tomko J, Paripati P, Orandle M, Kastenmayer RJ, Tartakovsky M, Rosenthal A, Portevin D, Eum SY, Lahouar S, Gagneux S, Young DB, Flynn JL, Barry CE 3rd. 2013. Differential virulence and disease progression following *Mycobacterium tuberculosis* complex infection of the common marmoset (*Callithrix jacchus*). *Infect Immun* **81**:2909–2919.
 23. Zumla A, George A, Sharma V, Herbert RH, Baroness Masham of Ilton, Oxley A, Oliver M. 2015. The WHO 2014 global tuberculosis report—further to go. *Lancet Glob Health* **3**:e10–e12.